



Inside dynamics for stage-structured integrodifference equations

Nathan G. Marculis¹ · Jimmy Garnier² · Roger Lui³ · Mark A. Lewis^{1,4}

Received: 30 May 2018 / Revised: 21 February 2019
© Springer-Verlag GmbH Germany, part of Springer Nature 2019

Abstract

A stage-structured model of integrodifference equations is used to study the asymptotic neutral genetic structure of populations undergoing range expansion. That is, we study the inside dynamics of solutions to stage-structured integrodifference equations. To analyze the genetic consequences for long term population spread, we decompose the solution into neutral genetic components called neutral fractions. The inside dynamics are then given by the spatiotemporal evolution of these neutral fractions. We show that, under some mild assumptions on the dispersal kernels and population projection matrix, the spread is dominated by individuals at the leading edge of the expansion. This result is consistent with the founder effect. In the case where there are multiple neutral fractions at the leading edge we are able to explicitly calculate the asymptotic proportion of these fractions found in the long-term population spread. This formula is simple and depends only on the right and left eigenvectors of the population projection matrix evaluated at zero and the initial proportion of each neutral fraction at the leading edge of the range expansion. In the absence of a strong Allee effect, multiple neutral fractions can drive the long-term population spread, a situation not possible with the scalar model.

Keywords Integrodifference equations · Stage-structure · Inside dynamics · Neutral genetic structure · Founder effect

Mathematics Subject Classification 39A10 · 45G10 · 92D25 · 92D40

✉ Nathan G. Marculis
marculis@ualberta.ca

¹ Department of Mathematical and Statistical Sciences, University of Alberta, Edmonton, AB T6G 2G1, Canada

² Université Savoie MontBlanc, CNRS, LAMA, F-73000 Chambéry, France

³ Department of Mathematical Sciences, Worcester Polytechnic Institute, Worcester, MA 01609, USA

⁴ Department of Biological Sciences, University of Alberta, Edmonton, AB T6G 2G1, Canada

1 Introduction

There are a wide array of observational (Cullingham et al. 2011), empirical (Liebhold et al. 1992; Lubina and Levin 1988), and theoretical studies (Li et al. 2009; Lui 1989a; Weinberger 1982) for the spatial spread of populations by range expansion. Over the last decades, theoretical studies about range expansion mainly focused on the asymptotic speed of propagation of the expanding population or the profile of invasion (Hastings et al. 2005). Spatial models in population genetics have also been developed for studying the spread of an advantageous gene in a population (Lui 1982a, b, 1983; Weinberger 1978, 1982). Recently, much effort have been invested to understand the genetic consequences of range expansion (Hallatschek and Nelson 2008; Roques et al. 2012). Indeed, range expansions are known to have significant effects on genetic diversity (Hewitt 2000; Davis and Shaw 2001). For instance, if range expansion occurs through successive founder effects, genetic diversity is likely to decrease. However, empirical and theoretical studies have shown that many mechanisms may reduce or reverse the loss of diversity in an expanding population (Pluess 2011). In particular, the presence of an Allee effect (Roques et al. 2012) which reduces the per-capita growth rate at low density, the occurrence of long distance dispersal events (Bonnefon et al. 2014; Ibrahim et al. 1996), or the existence of a juvenile stage (Austerlitz and Garnier-Géré 2003) may promote neutral genetic diversity in traveling waves of colonization. In this work, we are interested in the neutral genetic dynamics of a stage-structured population undergoing range expansion.

It is well known that the structure of the population is important for understanding the asymptotic dynamics. For example, individuals often must undergo a maturation period before they can produce offspring. For discrete population models, the dynamics of the life history traits have typically been structured according to age, Leslie matrix (Leslie 1945), or developmental stage, Lefkovitch matrix (Lefkovitch 1965), but matrix models can be easily generalized to include other physiological characteristics. It is also common for sessile species to typically have a motile stage in their development, such as seed dispersal in plant populations (Howe and Smallwood 1982) and larval dispersal in marine environments (Levin 2006).

Our study considers a stage-structured integrodifference equation describing range expansion for a population of the form:

$$\mathbf{u}_{t+1}(x) = \int_{-\infty}^{\infty} [\mathbf{K}(x - y) \circ \mathbf{B}(\mathbf{u}_t(y))] \mathbf{u}_t(y) dy, \quad (1)$$

where $\mathbf{u}_t(x)$ corresponds to the population density at time t and location x . The population is structured into m stages, whose densities are given by $\mathbf{u}_t(x) = [u_{1,t}(x), \dots, u_{m,t}(x)]$. Each stage distribution changes in time and space through the successive effects of dispersal, described by the dispersal matrix $\mathbf{K} = [k_{jl}]$, and the demography, embodied in the population projection matrix $\mathbf{B}(\mathbf{u}) = [b_{jl}(\mathbf{u})]$ which takes into account density-dependence. The succession of the reproduction stage and dispersal stage is described by the Hadamard product \circ (element-wise multiplication of matrix). This model allows the different stages to spread, reproduce, and interact in a variety of ways that cannot be captured by scalar models (Neubert and Caswell

2000). More precisely, if we consider stage j , where $j = 1, \dots, m$, then its density, $u_{j,t}(x)$, satisfies the following equation

$$u_{j,t+1} = \int_{-\infty}^{\infty} \sum_{l=1}^m k_{jl}(x-y) b_{jl}(u_{1,t}(y), \dots, u_{m,t}(y)) u_{l,t}(y) dy \quad (2)$$

where $k_{jl}(x-y) dy$ is the probability that an individual transitioning from stage l to stage j disperses from the interval $(y, y + dy]$ to location x , and the function b_{jl} is the per-capita production of stage j individuals from stage l individuals. Such a model has been used to describe epidemic spread (Lui 1989b), biological invasions (Bateman et al. 2017; Veit and Lewis 1996), and critical domain size (Lutscher and Lewis 2004).

The model (1) is biologically valid if the stages are chosen in a way such that the life history and dispersal parameters vary within stages as little as possible. In some cases this is easy; for example, a division between juvenile and adult individuals is normally determined by the ability to reproduce. In other cases, the division may not be so clear, and partitions may be difficult to decide. Fortunately, there are algorithms that can be used to minimize errors associated with partitioning a population into distinct stages (Moloney 1986; Vandermeer 1978). If the division of population structure is modeled using a continuous variable such as size or mass, and there is no natural break point to structure the population into distinct stages then an integral projection model may be more appropriate (Easterling et al. 2000).

The goal of this work is to understand the neutral genetic patterns of structured populations. Neutral genetic markers are genes that have no direct effect on individual fitness. Even though this type of gene tells us nothing about the adaptive or evolutionary potential of a population, neutral genetic markers can be used to understand processes such as gene flow, genetic drift, migration, or dispersal (Holderegger et al. 2006). It has also been shown by simulations that high levels of neutral genetic diversity can be correlated with increased allelic richness at loci under selection (Bataillon et al. 1996). Our analysis will be focused on the inside dynamics of stage-structured integrodifference equations.

This paper is organized as follows. Section 2 is dedicated to providing necessary background material for understanding the main results. Within this section, we break it into two subsections: Sect. 2.1 provides background to the analysis of inside dynamics and the stage-structured integrodifference equation used in our analysis and Sect. 2.2 lays out four of the major assumptions made about the demographic and dispersal processes. In Sect. 3, we provide asymptotic results regarding population structure. This section is broken into three parts. Section 3.1 covers the inside dynamics of neutral fractions not present at the leading edge, Sect. 3.2 discusses the inside dynamics of neutral fractions that are located at the leading edge, and Sect. 3.3 contains proofs for our main theorems. To complement the analytical results, numerical simulations are given in Sect. 4. Finally, in Sect. 5, we discuss the modeling technique, results, numerical simulations, and implications of our work.

2 Materials and methods

2.1 Inside dynamics

To study the neutral genetic distribution of a population, we consider the inside dynamics of the population. The term inside dynamics refers to the inside structure of the population rather than the total density. The key assumption in the analysis of inside dynamics is that all individuals grow and disperse in the same manner, differing only with respect to neutral genetic markers. In other words, all individuals in the population have the same fitness. This allows us to split up the population into distinct subgroups called neutral fractions with which we track the spatiotemporal evolution of these subgroups.

Inside dynamics have been studied for reaction-diffusion equations (Garnier and Lewis 2016; Garnier et al. 2012; Roques et al. 2012), delay reaction-diffusion equations (Bonneton et al. 2013), integro-differential equations (Bonneton et al. 2014), and integrodifference equations (Lewis et al. 2018; Marculis et al. 2017). In these works, the subject for analysis was a scalar population model. Indeed, to date, there is only one study of the inside dynamics of systems of equations. This study concentrated on the analysis on a diffusive Lotka-Volterra competition system (Roques et al. 2015). Our mathematical contribution to this area of research is to extend the analysis of inside dynamics to stage-structured integrodifference equations.

Recall the stage-structured population model in (1). Separating the initial population up into distinct neutral fractions, we obtain the initial condition

$$\mathbf{u}_0(x) = \sum_{i=1}^n \mathbf{v}_0^i(x), \quad (3)$$

where $\mathbf{v}_0^i(x) \geq 0$ is the initial population density for neutral fraction i and n is the finite number of neutral fractions. An illustration of this decomposition can be seen in Figs. 1a and 2a. By assuming that individuals in each neutral fraction grow and disperse similarly, we obtain the following system of equations:

$$\mathbf{v}_{t+1}^i(x) = \int_{-\infty}^{\infty} [\mathbf{K}(x-y) \circ \mathbf{B}(\mathbf{u}_t(y))] \mathbf{v}_t^i(y) dy, \quad i = 1, \dots, n, \quad (4)$$

where $\mathbf{u}_t(y) = \sum_{i=1}^n \mathbf{v}_t^i(y)$. Throughout the remaining sections, we use the superscript i to denote the neutral fraction and, when not written in vector form, subscript j to denotes the stage. Note that the number of neutral fractions, n , and the number of stages in the population, m , need not be the same ($n \neq m$). Also, observe the model given in Eq. (4) is natural extension of the scalar model to a system of recursions (Marculis et al. 2017). Thus, it can be expected that many of the results proven for the scalar equation can be extended to systems of cooperative equations. This is the approach we take in what follows.

2.2 Demographic and dispersal assumptions

For each of our main theorems, we make five assumptions regarding Eqs (3)–(4). The first three assumptions are related to the population projection matrix, the

fourth assumption is related to the dispersal kernel, and the fifth and final assumption is related to the decay of the initial conditions. In this section, we outline the first four assumptions related to the demography and dispersal of the population.

Population projection matrix

We begin with looking at the population projection matrix $\mathbf{B}(\mathbf{u})$. Here, we outline three assumptions about the population projection matrix. The population projection matrix describes reproduction, survival, and interactions between stages. As a projection matrix, its entries should be nonnegative:

A1: *The matrix $\mathbf{B}(\mathbf{u})$ is nonnegative for any $\mathbf{u} \in (0, \infty)^m$.*

Moreover, we can see from (1) that $\mathbf{0}$ is a steady state of the problem. Define

$$\mathbf{B}_0 := \mathbf{B}(\mathbf{u})|_{\mathbf{u}=\mathbf{0}}. \tag{5}$$

Notice that \mathbf{B}_0 is the population projection matrix evaluated at $\mathbf{u} = \mathbf{0}$. We will assume that this steady state is unstable. More precisely, we assume:

A2: *\mathbf{B}_0 is a primitive matrix, that is there exists $k > 0$ such that \mathbf{B}_0^k is positive, and its dominant eigenvalue, λ_1 , is greater than 1, $\lambda_1 > 1$.*

Finally, we assume that there are no Allee effects. That is:

A3: *$\mathbf{B}(\mathbf{u})$ is bounded by its linearization at the steady state $\mathbf{0}$, $\mathbf{B}(\mathbf{u})\mathbf{v} \leq \mathbf{B}_0\mathbf{v}$ for all $\mathbf{v} \in (0, \infty)^m$.*

Dispersal kernel

In our model, we assume that individuals in the population may disperse at long distance but those events are rare in the following sense:

Definition 1 A dispersal kernel, $k(x)$, is called *thin-tailed* if there exists a $\xi > 0$, such that

$$\int_{-\infty}^{\infty} k(x)e^{\xi|x|} dx < \infty. \tag{6}$$

A dispersal kernel that is not thin-tailed is called a fat-tailed dispersal kernel, and in this case, the long distance dispersal events become frequent, which leads to different behaviors for some solutions, such as accelerating waves. Many of the classical mathematical results for (1), such as traveling wave solutions and the asymptotic speed of propagation, rely on the assumption that the dispersal kernel is thin-tailed. A common dispersal kernel that we consider throughout our work is the Gaussian probability density function:

$$k(x; \mu, \sigma) = \frac{1}{\sqrt{2\pi\sigma^2}} e^{-\frac{(x-\mu)^2}{2\sigma^2}}, \tag{7}$$

where μ is the mean shift in location and σ^2 is the variance in dispersal distance. In the following sections, we use the following shorthand notation to denote that the dispersal kernel is Gaussian by k is $N(\mu, \sigma^2)$. In what follows, we will make one of two assumptions about the dispersal kernels.

A4: Each kernel, $k_{jl}(x - y)$, is thin-tailed.

A4': Each kernel, $k_{jl}(x - y)$, is $N(\mu, \sigma^2)$.

From above, we see that our fourth assumption provides a condition on the dispersal kernels. In both cases, we assume, at a minimum, that every dispersal kernel is thin-tailed in order to calculate the asymptotic speed of propagation. The above assumption implies that we are not considering a population with accelerating waves (Kot et al. 1996).

Asymptotic speed of propagation

Under the previous assumptions A1–A4 we can deduce from the work of Lui (1989a) that solutions of (1) will spread to the right with an asymptotic spreading speed c greater than or equal to a critical spreading speed $c^* > 0$ for appropriately chosen initial conditions. Moreover, the critical spreading speed c^* can be computed explicitly by the following formula

$$c^* := \min_{0 < s < s^+} \frac{1}{s} \ln \rho(s), \tag{8}$$

where $\rho(s) := \rho(\mathbf{H}(s)) > 1$ is the dominant eigenvalue of $\mathbf{H}(s)$ defined by

$$\mathbf{H}(s) := \mathbf{M}(s) \circ \mathbf{B}_0. \tag{9}$$

The moment generating function matrix $\mathbf{M}(s)$ is calculated by applying the reflected bilateral Laplace transform to the dispersal kernel matrix \mathbf{K} and is defined by

$$\mathbf{M}(s) := \int_{-\infty}^{\infty} \mathbf{K}(x) e^{sx} dx. \tag{10}$$

Since the entries of the dispersal kernel matrix, k_{jl} , are thin-tailed by Assumption A5, this matrix is well defined over $(0, s^+)$ where $s^+ \in (0, \infty]$. Throughout our analysis, we let $s_0(c)$ be the smallest positive root of the equation

$$cs = \ln(\rho(s)) \text{ for } c \geq c^*. \tag{11}$$

We know that $s_0(c)$ exists because $\rho(s)$ is log convex; see Lemma 6.4 by Lui (1989a). In particular, when each kernel is Gaussian, k_{jl} is $N(\mu, \sigma^2)$, then we have an explicit formula for the asymptotic speed of propagation given by

$$c^* = \sqrt{2\sigma^2 \ln(\lambda_1)} + \mu, \tag{12}$$

where λ_1 is the dominant eigenvalue of \mathbf{B}_0 and we can explicitly compute $s_0(c)$ to be

$$s_0(c) = \frac{c - \mu + \sqrt{(c - \mu)^2 - 2\sigma^2 \ln(\lambda_1)}}{\sigma^2}. \tag{13}$$

The technical details for the asymptotic speed of propagation are provided in Appendix A.

3 Main results

Henceforth, we assume that the structured population, $\mathbf{u}_t(x)$, satisfies (1) with an initial condition $\mathbf{u}_0(x)$. With such initial condition, the population is spreading to the right with an asymptotic speed of propagation, c , greater than or equal to c^* , given by formula (8). We first consider neutral fractions that are not present at the leading edge of the solution and then afterwards consider neutral fractions that are at the leading edge of the expanding population.

Our fifth and final assumption places a requirement on the initial conditions for the neutral fractions. This requirement is closely connected to the decay rate of the solution for the population and determines whether or not an individual is at the leading edge of the population spread. In particular, we know that the traveling wave solution for the linearized equation is given by an exponential function and the decay rate defines the leading edge of the population. The technical details of whether or not a neutral fraction is located at the leading edge is defined in the statement of our main theorems. We do not explicitly write these out here, but rather save them for the statement of our theorems because this assumption takes different forms based on our assumptions. We are now ready to present our first two theorems, that provides sufficient conditions for when the density of neutral fractions converges to zero in the moving half-frame.

3.1 Inside dynamics not at the leading edge

Theorem 3.1 *Let us assume that A1-A4 hold true. Let $\mathbf{v}_t^i(x)$ be a neutral fraction satisfying (4) with initial condition $\mathbf{v}_0^i(x)$ satisfying (3) that is not present at the leading edge of the expanding population, in the sense that*

$$A5: x^2 \mathbf{v}_0^i(x) e^{s_0(c)x} \in L^1(\mathbb{R}) \cap L^\infty(\mathbb{R}) \text{ for a given } c \geq c^*.$$

Then, for any $A \in \mathbb{R}$, the density of neutral fraction i , $\mathbf{v}_t^i(x)$, converges to $\mathbf{0}$ uniformly as $t \rightarrow \infty$ in the moving half-frame $[A + ct, \infty)$.

In summary, Theorem 3.1 provides sufficient conditions for neutral fractions in the population to approach zero asymptotically. This result implies that the only neutral fractions that will contribute to the spread of the population are those that are initially at the leading edge. In this scenario, we observe an extreme founder effect for the population spread. For this proof, see Sect. 3.3.

By making a stronger assumption on the dispersal kernels, we are able to relax Assumption A5 on the initial conditions in Theorem 3.1. In particular, for the next

theorem we assume that all dispersal kernels are Gaussian with the same mean and variance as given by Assumption A4' and the assumption on the initial condition becomes a simple integrability condition.

Theorem 3.2 *Let us assume that A1–A3 and A4' hold true. Let $v_t^i(x)$ be a neutral fraction satisfying (4) with initial condition $v_0^i(x)$ satisfying (3) that is not present at the leading edge of the expanding population, in the sense that*

$$A5': \int_{-\infty}^{\infty} e^{\frac{c-\mu}{\sigma^2}y} v_0^i(y) dy < \infty \text{ for a given } c \geq c^*.$$

Then, for any $A \in \mathbb{R}$, the density of neutral fraction i , $v_t^i(x)$, converges to $\mathbf{0}$ uniformly as $t \rightarrow \infty$ in the moving half-frame $[A + ct, \infty)$.

In summary, Theorem 3.2 provides the same result as Theorem 3.1 but with different assumptions on the dispersal kernels and initial conditions. That is, Theorem 3.2 provides sufficient conditions for when the neutral fractions do not contribute to the population spread. Under Assumption A5', we see that the leading edge is determined by the decaying exponential $e^{-\frac{c-\mu}{\sigma^2}x}$. This condition is much different than those given by Assumption A5 in Theorem 3.1. As in the previous theorem, we also observe here that the only neutral fractions that will contribute to the spread of the population are those that are initially at the leading edge. For this proof, see Sect. 3.3.

The proof of Theorem 3.1 is more complicated than that of Theorem 3.2, even though the method of proof and conclusions are the same. The difference is due to the assumptions made about the dispersal kernels. In Theorem 3.1 we assume the dispersal kernels are thin-tailed and must use the definition of the inverse reflected bilateral Laplace transform. In Theorem 3.2 we assume all dispersal kernels are Gaussian with the same mean and variance. This assumption simplifies the proof because convolving Gaussian distributions results in another Gaussian.

If the initial conditions are all compactly supported, then all neutral fractions will satisfy Assumption A5 and A5' respectively in Theorems 3.1 and 3.2. If the initial conditions decay according to the traveling wave solution, then all neutral fractions except those at the leading edge will satisfy Assumption A5 and A5' in Theorems 3.1 and 3.2 respectively. This means that the only neutral fractions that we will see in the moving half-frame are those that were initially at the leading edge. However, Theorems 3.1 and 3.2 do not tell us anything about these neutral fractions.

3.2 Inside dynamics at the leading edge

In the next theorem, we look at initial data that decay slower than Assumption A5' in Theorem 3.2. Here we are able to calculate the asymptotic proportion of each neutral fraction provided we move at the slowest speed c^* .

Theorem 3.3 *Let us assume that A1–A3 and A4' hold true. Let $v_t^i(x)$ be a neutral fraction satisfying (4) with initial condition $v_0^i(x)$ satisfying (3) that is present at the leading edge of the expanding population, in the sense that for $c = c^*$*

$$A5'': v_0^i(x) = (\mathbf{p}_0^i \circ \mathbf{r}) e^{-\frac{c-\mu}{\sigma^2}x}, \text{ where } \mathbf{p}_0^i \text{ is the initial proportion for neutral fraction } i \text{ in each stage, } \mathbf{r} \text{ is the right eigenvector of } \mathbf{B}_0 \text{ corresponding to } \lambda_1.$$

Then, for any $A \in \mathbb{R}$, the density of neutral fraction i , $\mathbf{v}_t^i(x)$, asymptotically approaches a proportion, p^i , of the traveling wave for the linear equation as $t \rightarrow \infty$ in the moving half-frame $[A + ct, \infty)$. That is,

$$\lim_{t \rightarrow \infty} \mathbf{v}_t^i(x_0 + ct) = e^{-\frac{c-\mu}{\sigma^2}x_0} \mathbf{r} p^i \tag{14}$$

for $x_0 \geq A$. Moreover, the proportion can be calculated to be the scalar

$$p^i = \boldsymbol{\ell} \left(\mathbf{p}_0^i \circ \mathbf{r} \right) \tag{15}$$

where $\boldsymbol{\ell}$ is the left eigenvector of \mathbf{B}_0 corresponding to λ_1 with $\boldsymbol{\ell}$ normalized by $\langle \boldsymbol{\ell}^T, \mathbf{r} \rangle$.

Theorem 3.3 provides a formula for the asymptotic proportion of neutral fractions based on the initial distribution at the leading edge of the population. The formula is simple because it depends only on the right and left eigenvectors of \mathbf{B}_0 and the initial proportion of neutral fractions. This theorem characterizes the fate of neutral fractions at the leading edge. One drawback to this theorem is that it is only valid for initial conditions that decay at a specific rate, $e^{-\frac{c-\mu}{\sigma^2}x}$, with a solution that moves at a specific speed, $c = c^*$. The reason why we cannot prove this theorem for $c > c^*$ and a slower decay rate for the initial condition is because we do not have an explicit formula for the spreading speed $c > c^*$. For this proof, see Sect. 3.3.

It is also important to note that $A5''$ in Theorem 3.3 is not completely biologically realistic since the population grows without bound as $x \rightarrow -\infty$. However, this type of initial condition is needed based on the construction of our sub-solution and super-solutions. It may be possible to relax this assumption by studying the nonlinear operator and considering a more biologically realistic class of initial conditions. Next, we present the proofs of Theorems 3.1–3.3 in Sect. 3.3. For a comprehensive review of the necessary mathematical material needed in the proofs of the theorems, we direct the reader to Appendix B.

3.3 Proofs of the main theorems

Proof of Theorem 3.1

Proof For simplicity, we drop the superscript i in (4) and focus on a single neutral fraction. Our equation of interest is

$$\mathbf{v}_{t+1}(x) = \int_{-\infty}^{\infty} [\mathbf{K}(x - y) \circ \mathbf{B}(\mathbf{u}_t(y))] \mathbf{v}_t(y) dy. \tag{16}$$

Let

$$\mathbf{w}_0(x) = \frac{\mathbf{C}e^{-s_0(c)x}}{1 + x^2} \tag{17}$$

where $\mathbf{C} = \kappa\phi$ and ϕ is the eigenvector of $\mathbf{H}(s_0(c))$ with dominant eigenvalue $\rho(s_0(c))$. From Lemma B.1, we know that $\mathbf{w}_0(x)$ is an upper bound for $\mathbf{v}_0(x)$. By Assumption A3, we know that $\mathbf{B}(\mathbf{u}_t(y))\mathbf{v} \leq \mathbf{B}_0\mathbf{v}$ for all $\mathbf{v} \geq 0$. Hence, we can construct a super-solution $\mathbf{w}_t(x)$ that satisfies the following equation

$$\mathbf{w}_{t+1}(x) = \int_{-\infty}^{\infty} [\mathbf{K}(x - y) \circ \mathbf{B}_0] \mathbf{w}_t(y) dy \tag{18}$$

with initial condition given by (17). By iterating we can write the solution to the above system as the t -fold convolution

$$\mathbf{w}_t(x) = [\mathbf{K}(x - y) \circ \mathbf{B}_0]^{*t} \mathbf{w}_0(y). \tag{19}$$

Applying the bilateral Laplace transform

$$\mathbf{W}_t(s) = [\mathbf{M}(s) \circ \mathbf{B}_0]^t \mathbf{W}_0(s) \tag{20}$$

$$= [\mathbf{H}(s)]^t \mathbf{W}_0(s). \tag{21}$$

Recall that $s_0(c)$ is the smallest positive root of $sc = \ln(\rho(s))$ for $c \geq c^*$. Then, the inverse transform as defined in Appendix B, see (130), yields

$$\mathbf{w}_t(x) = \frac{1}{2\pi i} \lim_{R \rightarrow \infty} \int_{s_0(c)-iR}^{s_0(c)+iR} [\mathbf{H}(s)]^t \mathbf{W}_0(s) e^{-sx} ds \tag{22}$$

$$= \frac{1}{2\pi} \int_{-\infty}^{\infty} [\mathbf{H}(s_0(c) + i\omega)]^t \mathbf{W}_0(s_0(c) + i\omega) e^{-(s_0(c)+i\omega)x} d\omega \tag{23}$$

for $c \geq c^*$. In the moving frame we have

$$\mathbf{w}_t(x_0 + ct) = \frac{1}{2\pi} \int_{-\infty}^{\infty} [\mathbf{H}(s_0(c) + i\omega)]^t \mathbf{W}_0(s_0(c) + i\omega) e^{-(s_0(c)+i\omega)x_0} e^{-(s_0(c)+i\omega)ct} d\omega. \tag{24}$$

Using the results from Lemma B.1, see Appendix B for details, we are able to write the initial condition in terms of a Fourier transform that is known. This is seen as follows,

$$\mathbf{W}_0(s_0(c) + i\omega) = \int_{-\infty}^{\infty} \mathbf{w}_0(x) e^{(s_0(c)+i\omega)x} dx \tag{25}$$

$$= \int_{-\infty}^{\infty} \mathbf{w}_0(x) e^{s_0(c)x} e^{i\omega x} dx \tag{26}$$

$$= \mathcal{F} \left[\mathbf{w}_0(x) e^{s_0(c)x} \right] (-\omega) \tag{27}$$

$$= \mathbf{C}\pi e^{-|\omega|} \tag{28}$$

for all $\omega \in \mathbb{R}$. Recall that $\mathbf{C} = \kappa \boldsymbol{\phi}$. This gives

$$\mathbf{w}_t(x_0 + ct) = \frac{1}{2\pi} \int_{-\infty}^{\infty} [\mathbf{H}(s_0(c) + i\omega)]^t \mathbf{C} \pi e^{-|\omega|} e^{-(s_0(c)+i\omega)x_0} e^{-(s_0(c)+i\omega)ct} d\omega \tag{29}$$

$$= \frac{1}{2} \int_{-\infty}^{\infty} [\mathbf{H}(s_0(c) + i\omega)]^t \kappa e^{-s_0(c)ct} \boldsymbol{\phi} e^{-|\omega|} e^{-(s_0(c)+i\omega)x_0} e^{-i\omega ct} d\omega. \tag{30}$$

Since $s_0(c)c = \ln(\rho(s_0(c)))$, we have

$$\mathbf{w}_t(x_0 + ct) = \frac{\kappa e^{-s_0(c)x_0}}{2} \int_{-\infty}^{\infty} [\mathbf{H}(s_0(c) + i\omega)]^t e^{-\ln(\rho(s_0(c)))t} \boldsymbol{\phi} e^{-|\omega|} e^{-i\omega x_0} e^{-i\omega ct} d\omega \tag{31}$$

$$= \frac{\kappa e^{-s_0(c)x_0}}{2} \int_{-\infty}^{\infty} [\mathbf{H}(s_0(c) + i\omega)]^t (\rho(s_0(c)))^{-t} \boldsymbol{\phi} e^{-|\omega|} e^{-i\omega x_0} e^{-i\omega ct} d\omega. \tag{32}$$

Since $\rho(s_0(c))$ is the dominant eigenvalue of $\mathbf{H}(s_0(c))$ with eigenvector $\boldsymbol{\phi}$,

$$\mathbf{w}_t(x_0 + ct) = \frac{\kappa e^{-s_0(c)x_0}}{2} \int_{-\infty}^{\infty} [\mathbf{H}(s_0(c) + i\omega)]^t [\mathbf{H}(s_0(c))]^{-t} \boldsymbol{\phi} e^{-|\omega|} e^{-i\omega x_0} e^{-i\omega ct} d\omega. \tag{33}$$

Applying the matrix norm and using the sub-additive property, we find that

$$\|\mathbf{w}_t(x_0 + ct)\| \leq \frac{\kappa e^{-s_0(c)x_0}}{2} \int_{-\infty}^{\infty} \|[\mathbf{H}(s_0(c) + i\omega)]^t\| \|[\mathbf{H}(s_0(c))]^{-t}\| \|\boldsymbol{\phi}\| e^{-|\omega|} |e^{-i\omega x_0}| |e^{-i\omega ct}| d\omega \tag{34}$$

$$= \frac{\kappa e^{-s_0(c)x_0}}{2} \int_{-\infty}^{\infty} \|[\mathbf{H}(s_0(c) + i\omega)]^t\| \|[\mathbf{H}(s_0(c))]^{-t}\| \|\boldsymbol{\phi}\| e^{-|\omega|} d\omega. \tag{35}$$

We can also see that

$$|\mathbf{H}(s_0(c) + i\omega)| = |\mathbf{M}(s_0(c) + i\omega) \circ \mathbf{B}_0| \tag{36}$$

$$= \left| \int_{-\infty}^{\infty} [\mathbf{K}(x) \circ \mathbf{B}_0] e^{(s_0(c)+i\omega)x} dx \right| \tag{37}$$

$$= \left| \int_{-\infty}^{\infty} [\mathbf{K}(x) \circ \mathbf{B}_0] e^{s_0(c)x} (\cos(\omega x) + i \sin(\omega x)) dx \right| \tag{38}$$

$$= I, \tag{39}$$

where I is defined to be

$$I := \sqrt{\left(\int_{-\infty}^{\infty} [\mathbf{K}(x) \circ \mathbf{B}_0] e^{s_0(c)x} \cos(\omega x) dx\right)^2 + \left(\int_{-\infty}^{\infty} [\mathbf{K}(x) \circ \mathbf{B}_0] e^{s_0(c)x} \sin(\omega x) dx\right)^2}. \tag{40}$$

By the Cauchy-Schwarz inequality, using a similar technique as in Theorem 3 of (Marculis et al. 2017),

$$I < \int_{-\infty}^{\infty} [\mathbf{K}(x) \circ \mathbf{B}_0] e^{s_0(c)x} dx \tag{41}$$

$$= \mathbf{M}(s_0(c)) \circ \mathbf{B}_0 \tag{42}$$

$$= \mathbf{H}(s_0(c)) \tag{43}$$

for $\omega \neq 0$. From the above calculation we can conclude that $|\mathbf{H}(s_0(c) + i\omega)| < \mathbf{H}(s_0(c))$ for $\omega \neq 0$. Consequently, $\rho(|\mathbf{H}(s_0(c) + i\omega)|) < \rho(s_0(c))$ for $\omega \neq 0$. By Gelfand’s formula,

$$\lim_{t \rightarrow \infty} \left\| \left[\mathbf{H}(s_0(c) + i\omega) \right]^t \right\|^{1/t} = \rho(|\mathbf{H}(s_0(c) + i\omega)|) \quad \text{and} \tag{44}$$

$$\lim_{t \rightarrow \infty} \left\| \left[\mathbf{H}(s_0(c)) \right]^{-t} \right\|^{1/t} = \frac{1}{\rho(s_0(c))}. \tag{45}$$

Thus, for $\omega \neq 0$, we can choose $\varepsilon > 0$ such that $(\rho(|\mathbf{H}(s_0(c) + i\omega)|) + \varepsilon) \left(\frac{1}{\rho(s_0(c))} + \varepsilon\right) < 1$. Therefore,

$$\left\| \left[\mathbf{H}(s_0(c) + i\omega) \right]^t \right\| \left\| \left[\mathbf{H}(s_0(c)) \right]^{-t} \right\| < 1 \tag{46}$$

for large t and

$$\lim_{t \rightarrow \infty} \left\| \left[\mathbf{H}(s_0(c) + i\omega) \right]^t \right\| \left\| \left[\mathbf{H}(s_0(c)) \right]^{-t} \right\| = 0. \tag{47}$$

From (35) and the dominated convergence theorem,

$$\begin{aligned} & \lim_{t \rightarrow \infty} \|\mathbf{w}_t(x_0 + ct)\| \\ & \leq \frac{\kappa e^{-s_0(c)x_0}}{2} \int_{-\infty}^{\infty} \lim_{t \rightarrow \infty} \left\| \left[\mathbf{H}(s_0(c) + i\omega) \right]^t \right\| \left\| \left[\mathbf{H}(s_0(c)) \right]^{-t} \right\| \|\phi\| e^{-|\omega|} d\omega \end{aligned} \tag{48}$$

$$= \mathbf{0}. \tag{49}$$

Therefore, for any $A \in \mathbb{R}$ and $c \geq c^*$,

$$\lim_{t \rightarrow \infty} \max_{[A, \infty)} \mathbf{w}_t(x + ct) = \mathbf{0}. \tag{50}$$

Since \mathbf{w} was constructed as a super-solution, we can conclude that

$$\lim_{t \rightarrow \infty} \max_{[A, \infty)} \mathbf{v}_t(x + ct) = \mathbf{0}. \tag{51}$$

The proof of Theorem 3.1 is complete. □

Proof of Theorem 3.2

Proof For simplicity, we focus on a single neutral fraction and drop the superscript i . By Assumption A3, $\mathbf{B}(\mathbf{u}_t(y))\mathbf{v} \leq \mathbf{B}_0\mathbf{v}$ for all $\mathbf{v} \geq 0$, we can use a comparison principle to show that a new sequence $\mathbf{w}_t(x)$ defined by

$$\mathbf{w}_{t+1}(x) = \int_{-\infty}^{\infty} [\mathbf{K}(x - y) \circ \mathbf{B}_0] \mathbf{w}_t(y) dy \tag{52}$$

is always greater than the solution to any neutral fraction $\mathbf{v}_t(x)$ with the same initial condition, $\mathbf{w}_0(x) = \mathbf{v}_0(x)$. By iterating we can write the solution to Eq. (52) as the t -fold convolution

$$\mathbf{w}_t(x) = [\mathbf{K}(x - y) \circ \mathbf{B}_0]^{*t} \mathbf{w}_0(y). \tag{53}$$

Taking the bilateral Laplace transform

$$\mathcal{M}[\mathbf{w}_t(x)](s) = [\mathcal{M}[\mathbf{K}(x)](s) \circ \mathbf{B}_0]^t \mathcal{M}[\mathbf{w}_0(x)](s). \tag{54}$$

Since all of the dispersal kernels are Gaussian, we know that $\mathcal{M}[\mathbf{K}(x)](s) = e^{\frac{\sigma^2 s^2}{2} + \mu s} \mathbf{1}$ where $\mathbf{1}$ is a matrix of all ones. Then,

$$\begin{aligned} & [\mathcal{M}[\mathbf{K}(x)](s) \circ \mathbf{B}_0]^t \mathcal{M}[\mathbf{w}_0(x)](s) \\ &= \left[e^{\frac{\sigma^2 s^2}{2} + \mu s} \mathbf{1} \circ \mathbf{B}_0 \right]^t \mathcal{M}[\mathbf{w}_0(x)](s) \end{aligned} \tag{55}$$

$$= \left[e^{\frac{\sigma^2 s^2}{2} + \mu s} \mathbf{B}_0 \right]^t \mathcal{M}[\mathbf{w}_0(x)](s) \tag{56}$$

$$= e^{\frac{\sigma^2 t s^2}{2} + \mu t s} [\mathbf{B}_0]^t \mathcal{M}[\mathbf{w}_0(x)](s) \tag{57}$$

$$= [\mathbf{B}_0]^t \mathcal{M} \left[\frac{1}{\sqrt{2\pi\sigma^2 t}} e^{-\frac{(x-\mu t)^2}{2\sigma^2 t}} \right] (s) \mathcal{M}[\mathbf{w}_0(x)](s) \tag{58}$$

$$= [\mathbf{B}_0]^t \mathcal{M} [(K_t * \mathbf{w}_0)(x)] (s) \tag{59}$$

where K_t is $N(\mu t, \sigma^2 t)$. From (54)

$$\mathcal{M}[\mathbf{w}_t(x)](s) = [\mathbf{B}_0]^t \mathcal{M} [(K_t * \mathbf{w}_0)(x)] (s). \tag{60}$$

Applying the inverse bilateral Laplace transform,

$$\mathbf{w}_t(x) = [\mathbf{B}_0]^t (K_t * \mathbf{w}_0)(x) \tag{61}$$

$$= [\mathbf{B}_0]^t \int_{-\infty}^{\infty} \frac{1}{\sqrt{2\pi\sigma^2t}} e^{-\frac{(x-y-\mu t)^2}{2\sigma^2t}} \mathbf{w}_0(y) dy \tag{62}$$

In the moving half-frame $[A + ct, \infty)$ with $c \geq c^*$ we have

$$\mathbf{w}_t(x_0 + ct) = [\mathbf{B}_0]^t \int_{-\infty}^{\infty} \frac{1}{\sqrt{2\pi\sigma^2t}} e^{-\frac{(x_0+ct-y-\mu t)^2}{2\sigma^2t}} \mathbf{w}_0(y) dy. \tag{63}$$

From (12), we know that $c^* = \sqrt{2\sigma^2 \ln(\lambda_1)} + \mu$, expanding the exponent, yields

$$\frac{(x_0 + ct - y - \mu t)^2}{2\sigma^2t} = \frac{(x_0 - y)^2}{2\sigma^2t} + \frac{2(c - \mu)t(x_0 - y) + (c - \mu)^2t^2}{2\sigma^2t} \tag{64}$$

$$\geq \frac{(x_0 - y)^2}{2\sigma^2t} + \frac{c - \mu}{\sigma^2}(x_0 - y) + \ln(\lambda_1)t. \tag{65}$$

Thus,

$$\mathbf{w}_t(x_0 + ct) \leq \frac{[\mathbf{B}_0]^t}{\sqrt{2\pi\sigma^2t}} \int_{-\infty}^{\infty} e^{-\frac{(x_0-y)^2}{2\sigma^2t}} e^{-\frac{c-\mu}{\sigma^2}(x_0-y)} e^{-\ln(\lambda_1)t} \mathbf{w}_0(y) dy \tag{66}$$

$$= \left[\frac{\mathbf{B}_0}{\lambda_1} \right]^t \frac{1}{\sqrt{2\pi\sigma^2t}} \int_{-\infty}^{\infty} e^{-\frac{(x_0-y)^2}{2\sigma^2t}} e^{-\frac{c-\mu}{\sigma^2}(x_0-y)} \mathbf{w}_0(y) dy. \tag{67}$$

Since $x_0 \geq A$ and $e^{-\frac{(x_0-y)^2}{2\sigma^2t}} \leq 1$, we have

$$\mathbf{w}_t(x_0 + ct) \leq \left[\frac{\mathbf{B}_0}{\lambda_1} \right]^t \frac{e^{-\frac{A(c-\mu)}{\sigma^2}}}{\sqrt{2\pi\sigma^2t}} \int_{-\infty}^{\infty} e^{\frac{c-\mu}{\sigma^2}y} \mathbf{w}_0(y) dy. \tag{68}$$

From Lemma B.2, see Appendix B for details, we know that

$$\lim_{t \rightarrow \infty} \left[\frac{\mathbf{B}_0}{\lambda_1} \right]^t = \mathbf{r}\ell, \tag{69}$$

where \mathbf{r} and ℓ are the right and left eigenvectors of \mathbf{B}_0 corresponding to λ_1 respectively with ℓ normalized by $\langle \ell^T, \mathbf{r} \rangle$ to account for the scaling in \mathbf{r} . Note that $\mathbf{r}\ell$ is a $m \times m$ matrix since \mathbf{r} is $m \times 1$ and ℓ is $1 \times m$. Thus since $\int_{-\infty}^{\infty} e^{\frac{c-\mu}{\sigma^2}y} \mathbf{w}_0(y) dy < \infty$ by Assumption A5' and (69) we have $\mathbf{w}_t(x_0 + ct) \rightarrow \mathbf{0}$ uniformly as $t \rightarrow \infty$ in $[A, \infty)$. Recall that $\mathbf{w}_t(x)$ was a constructed as a super-solution, $\mathbf{0} \leq \mathbf{v}_t(x) \leq \mathbf{w}_t(x)$. This implies the uniform convergence of $\mathbf{v}_t(x) \rightarrow \mathbf{0}$ as $t \rightarrow \infty$ in the moving half-frame $[A + ct, \infty)$. The proof of Theorem 3.2 is complete. \square

Proof of Theorem 3.3

Proof For simplicity, we focus on a single neutral fraction and drop the superscript i . Using the fact that $\mathbf{B}(\mathbf{u}_t(y))\mathbf{v} \leq \mathbf{B}_0\mathbf{v}$ for all $\mathbf{v} \geq 0$ we can use a comparison principle to show that a new sequence $\mathbf{w}_t(x)$ defined by

$$\mathbf{w}_{t+1}(x) = \int_{-\infty}^{\infty} [\mathbf{K}(x - y) \circ \mathbf{B}_0] \mathbf{w}_t(y) dy \tag{70}$$

is a super-solution to any neutral fraction $\mathbf{v}_t(x)$ with the same initial condition $\mathbf{w}_0(x) = \mathbf{v}_0(x)$. By iterating we can write the solution to Eq. (70) as the t -fold convolution

$$\mathbf{w}_t(x) = [\mathbf{K}(x - y) \circ \mathbf{B}_0]^{*t} \mathbf{w}_0(y). \tag{71}$$

Taking the bilateral Laplace transform

$$\mathcal{M}[\mathbf{w}_t(x)](s) = [\mathcal{M}[\mathbf{K}(x)](s) \circ \mathbf{B}_0]^t \mathcal{M}[\mathbf{w}_0(x)](s). \tag{72}$$

Since all of the dispersal kernels are Gaussian, we know that $\mathcal{M}[\mathbf{K}(x)](s) = e^{\frac{\sigma^2 s^2}{2} + \mu s} \mathbf{1}$ where $\mathbf{1}$ is a matrix of all ones. Then, we can see that

$$\begin{aligned} & [\mathcal{M}[\mathbf{K}(x)](s) \circ \mathbf{B}_0]^t \mathcal{M}[\mathbf{w}_0(x)](s) \\ &= \left[e^{\frac{\sigma^2 s^2}{2} + \mu s} \mathbf{1} \circ \mathbf{B}_0 \right]^t \mathcal{M}[\mathbf{w}_0(x)](s) \end{aligned} \tag{73}$$

$$= \left[e^{\frac{\sigma^2 s^2}{2} + \mu s} \mathbf{B}_0 \right]^t \mathcal{M}[\mathbf{w}_0(x)](s) \tag{74}$$

$$= e^{\frac{\sigma^2 t s^2}{2} + \mu t s} \mathbf{I} [\mathbf{B}_0]^t \mathcal{M}[\mathbf{w}_0(x)](s) \tag{75}$$

$$= [\mathbf{B}_0]^t \mathcal{M} \left[\frac{1}{\sqrt{2\pi\sigma^2 t}} e^{-\frac{(x-\mu t)^2}{2\sigma^2 t}} \mathbf{I} \right] (s) \mathcal{M}[\mathbf{w}_0(x)](s) \tag{76}$$

$$= [\mathbf{B}_0]^t \mathcal{M} [(\mathbf{K}_t * \mathbf{w}_0)(x)] (s) \tag{77}$$

where \mathbf{K}_t is a diagonal matrix with $N(\mu t, \sigma^2 t)$ entries and \mathbf{I} is the identity matrix. Thus, we have

$$\mathcal{M}[\mathbf{w}_t(x)](s) = [\mathbf{B}_0]^t \mathcal{M} [(\mathbf{K}_t * \mathbf{w}_0)(x)] (s). \tag{78}$$

Then applying the inverse transform yields

$$\mathbf{w}_t(x) = [\mathbf{B}_0]^t (\mathbf{K}_t * \mathbf{w}_0)(x) \tag{79}$$

$$= [\mathbf{B}_0]^t \int_{-\infty}^{\infty} \frac{1}{\sqrt{2\pi\sigma^2 t}} e^{-\frac{(x-y-\mu t)^2}{2\sigma^2 t}} \mathbf{w}_0(y) dy \tag{80}$$

In the moving half-frame $[A + ct, \infty)$ with fixed $A \in \mathbb{R}$, consider the element $x_0 + ct$ with $c = c^* = \sqrt{2\sigma^2 \ln(\lambda_1)} + \mu$ where λ_1 is the dominant eigenvalue of \mathbf{B}_0 as given by (12). By rewriting $\mathbf{w}_t(x)$ in this moving half-frame we have

$$\mathbf{w}_t(x_0 + ct) = [\mathbf{B}_0]^t \int_{-\infty}^{\infty} \frac{1}{\sqrt{2\pi\sigma^2 t}} e^{-\frac{(x_0+ct-y-\mu t)^2}{2\sigma^2 t}} \mathbf{w}_0(y) dy. \tag{81}$$

Expanding the exponent, yields

$$\frac{(x_0 + ct - y - \mu t)^2}{2\sigma^2 t} = \frac{(y - x_0)^2}{2\sigma^2 t} + \frac{(c - \mu)(x_0 - y)}{\sigma^2} + \frac{(c - \mu)^2}{2\sigma^2} t. \tag{82}$$

Thus,

$$\begin{aligned} \mathbf{w}_t(x_0 + ct) &= \frac{[\mathbf{B}_0]^t}{\sqrt{2\pi\sigma^2 t}} \int_{-\infty}^{\infty} e^{-\frac{(y-x_0)^2}{2\sigma^2 t}} e^{-\frac{(c-\mu)(x_0-y)}{\sigma^2}} e^{-\frac{(c-\mu)^2}{2\sigma^2} t} \mathbf{w}_0(y) dy \end{aligned} \tag{83}$$

$$= \left[\frac{\mathbf{B}_0}{\lambda_1} \right]^t \frac{1}{\sqrt{2\pi\sigma^2 t}} \int_{-\infty}^{\infty} e^{-\frac{(y-x_0)^2}{2\sigma^2 t}} e^{-\frac{(c-\mu)(x_0-y)}{\sigma^2}} e^{\left[-\frac{(c-\mu)^2}{2\sigma^2} + \ln(\lambda_1) \right] t} \mathbf{w}_0(y) dy. \tag{84}$$

Since $c = c^* = \sqrt{2\sigma^2 \ln(\lambda_1)} + \mu$, we have that

$$\mathbf{w}_t(x_0 + ct) = \left[\frac{\mathbf{B}_0}{\lambda_1} \right]^t \frac{1}{\sqrt{2\pi\sigma^2 t}} \int_{-\infty}^{\infty} e^{-\frac{(y-x_0)^2}{2\sigma^2 t}} e^{-\frac{(c-\mu)(x_0-y)}{\sigma^2}} \mathbf{w}_0(y) dy. \tag{85}$$

From Assumption A5'', $\mathbf{w}_0(y) = (\mathbf{p}_0 \circ \mathbf{r}) e^{-\frac{c-\mu}{\sigma^2} y}$. Thus,

$$\mathbf{w}_t(x_0 + ct) = \left[\frac{\mathbf{B}_0}{\lambda_1} \right]^t (\mathbf{p}_0 \circ \mathbf{r}) e^{-\frac{(c-\mu)}{\sigma^2} x_0} \frac{1}{\sqrt{2\pi\sigma^2 t}} \int_{-\infty}^{\infty} e^{-\frac{(y-x_0)^2}{2\sigma^2 t}} dy \tag{86}$$

$$= \left[\frac{\mathbf{B}_0}{\lambda_1} \right]^t (\mathbf{p}_0 \circ \mathbf{r}) e^{-\frac{(c-\mu)}{\sigma^2} x_0}. \tag{87}$$

From Lemma B.2, see Appendix B for details, we know that

$$\lim_{t \rightarrow \infty} \left[\frac{\mathbf{B}_0}{\lambda_1} \right]^t = \mathbf{r} \boldsymbol{\ell} \tag{88}$$

where \mathbf{r} and $\boldsymbol{\ell}$ are the right and left eigenvectors of \mathbf{B}_0 corresponding to λ_1 respectively where $\boldsymbol{\ell}$ is normalized by $(\boldsymbol{\ell}^T, \mathbf{r})$. Thus,

$$\lim_{t \rightarrow \infty} \mathbf{w}_t(x_0 + ct) = \lim_{t \rightarrow \infty} \left[\frac{\mathbf{B}_0}{\lambda_1} \right]^t (\mathbf{p}_0 \circ \mathbf{r}) e^{-\frac{(c-\mu)}{\sigma^2} x_0} \tag{89}$$

$$= \mathbf{r}\ell (\mathbf{p}_0 \circ \mathbf{r}) e^{-\frac{(c-\mu)}{\sigma^2}x_0} \tag{90}$$

$$= e^{-\frac{(c-\mu)}{\sigma^2}x_0} \mathbf{r}p. \tag{91}$$

From the above calculations, we find that the super-solution approaches a proportion, p , of the traveling wave for the linear equation where $p = \ell (\mathbf{p}_0 \circ \mathbf{r})$. We now move onto our sub-solution. For any $0 < \varepsilon \ll 1$, δ is chosen such that $(1 - \varepsilon)\mathbf{B}_0\delta = \mathbf{B}(\delta)\delta$ and we define

$$(\mathbf{B}_{sub}(\mathbf{u}; \varepsilon))_{jl} := \begin{cases} (1 - \varepsilon) (\mathbf{B}(\mathbf{u}))_{jl} & \text{if } (\mathbf{B}(\mathbf{u}))_{jl} \text{ is constant} \\ \beta_{jl}(\mathbf{u}; \varepsilon) & \text{if } (\mathbf{B}(\mathbf{u}))_{jl} \text{ is non-constant,} \end{cases} \tag{92}$$

where

$$\beta_{jl}(\mathbf{u}; \varepsilon) := \begin{cases} (1 - \varepsilon) (\mathbf{B}_0)_{jl} & \text{for } 0 \leq \mathbf{u} < \delta \\ (\mathbf{B}(\mathbf{u}))_{jl} & \text{for } \mathbf{u} \geq \delta. \end{cases} \tag{93}$$

Then,

$$\mathbf{z}_{t+1}(x) = \int_{-\infty}^{\infty} [\mathbf{K}(x - y) \circ \mathbf{B}_{sub}(\mathbf{u}_t(y); \varepsilon)] \mathbf{z}_t(y) dy \tag{94}$$

with $\mathbf{z}_0(x) = \mathbf{v}_0(x)$ is a sub-solution of $\mathbf{v}_t(x)$ by the comparison principle since $\mathbf{B}_{sub}(\mathbf{u}; \varepsilon)\mathbf{v} \leq \mathbf{B}(\mathbf{u})\mathbf{v}$ for all $\mathbf{v} \geq 0$. Define $c(\varepsilon) := \sqrt{2\sigma^2 \ln((1 - \varepsilon)\lambda_1) + \mu}$ where $(1 - \varepsilon)\lambda_1$ is the dominant eigenvalue of the constant matrix $(1 - \varepsilon)\mathbf{B}_0$. In the moving half-frame $[A + c(\varepsilon)t, \infty)$ with fixed $A \in \mathbb{R}$, choose x_0 large such that $\mathbf{u}_t(y)$ in (94) satisfies $\mathbf{u}_t(y) < \delta$ for all t where $y \in [x_0 + c(\varepsilon)t, \infty)$. Then by the definition of $\mathbf{B}_{sub}(\mathbf{u}; \varepsilon)$

$$\mathbf{z}_{t+1}(x_0 + c(\varepsilon)t) = \int_{-\infty}^{\infty} [\mathbf{K}(x_0 + c(\varepsilon)t - y) \circ (1 - \varepsilon)\mathbf{B}_0] \mathbf{z}_t(y) dy. \tag{95}$$

By iterating we can write the solution to (95) as the t -fold convolution

$$\mathbf{z}_t(x_0 + c(\varepsilon)t) = [\mathbf{K}(x_0 + c(\varepsilon)t - y) \circ (1 - \varepsilon)\mathbf{B}_0]^{*t} \mathbf{z}_0(y). \tag{96}$$

Since we assumed that all of the dispersal kernels are Gaussian, by repeating calculations done previously we find that

$$\mathbf{z}_t(x_0 + c(\varepsilon)t) = [(1 - \varepsilon)\mathbf{B}_0]^t \int_{-\infty}^{\infty} \frac{1}{\sqrt{2\pi\sigma^2t}} e^{-\frac{(x_0+c(\varepsilon)t-y-\mu t)^2}{2\sigma^2t}} \mathbf{z}_0(y) dy \tag{97}$$

$$= \frac{[(1 - \varepsilon)\mathbf{B}_0]^t}{\sqrt{2\pi\sigma^2t}} \int_{-\infty}^{\infty} e^{-\frac{(x_0-y)^2}{2\sigma^2t}} e^{-\frac{(c(\varepsilon)-\mu)(x_0-y)}{\sigma^2}} e^{-\frac{(c(\varepsilon)-\mu)^2}{2\sigma^2}t} \mathbf{z}_0(y) dy \tag{98}$$

$$\begin{aligned}
 &= \left[\frac{(1 - \varepsilon)\mathbf{B}_0}{(1 - \varepsilon)\lambda_1} \right]^t \frac{1}{\sqrt{2\pi\sigma^2t}} \\
 &\int_{-\infty}^{\infty} e^{-\frac{(x_0-y)^2}{2\sigma^2t}} e^{-\frac{(c(\varepsilon)-\mu)(x_0-y)}{\sigma^2}} e^{\left[-\frac{(c(\varepsilon)-\mu)^2}{2\sigma^2} + \ln((1-\varepsilon)\lambda_1) \right]t} \mathbf{z}_0(y) dy \quad (99) \\
 &= \left[\frac{\mathbf{B}_0}{\lambda_1} \right]^t \frac{1}{\sqrt{2\pi\sigma^2t}} \\
 &\int_{-\infty}^{\infty} e^{-\frac{(x_0-y)^2}{2\sigma^2t}} e^{-\frac{(c(\varepsilon)-\mu)(x_0-y)}{\sigma^2}} e^{\left[-\frac{(c(\varepsilon)-\mu)^2}{2\sigma^2} + \ln((1-\varepsilon)\lambda_1) \right]t} \mathbf{z}_0(y) dy.
 \end{aligned}$$

(100)

Since $c(\varepsilon) = \sqrt{2\sigma^2 \ln((1 - \varepsilon)\lambda_1)} + \mu$,

$$\mathbf{z}_t(x_0 + c(\varepsilon)t) = \left[\frac{\mathbf{B}_0}{\lambda_1} \right]^t \frac{1}{\sqrt{2\pi\sigma^2t}} \int_{-\infty}^{\infty} e^{-\frac{(x_0-y)^2}{2\sigma^2t}} e^{-\frac{(c(\varepsilon)-\mu)(x_0-y)}{\sigma^2}} \mathbf{z}_0(y) dy. \quad (101)$$

Note that the integrand in (101) is nonnegative and integrable. Using Fatou’s lemma we fix t and let $\varepsilon \rightarrow 0$, giving

$$\mathbf{z}_t(x_0 + ct) = \liminf_{\varepsilon \rightarrow 0} \mathbf{z}_t(x_0 + c(\varepsilon)t) \quad (102)$$

$$= \liminf_{\varepsilon \rightarrow 0} \left[\frac{\mathbf{B}_0}{\lambda_1} \right]^t \frac{1}{\sqrt{2\pi\sigma^2t}} \int_{-\infty}^{\infty} e^{-\frac{(x_0-y)^2}{2\sigma^2t}} e^{-\frac{(c(\varepsilon)-\mu)(x_0-y)}{\sigma^2}} \mathbf{z}_0(y) dy \quad (103)$$

$$\geq \left[\frac{\mathbf{B}_0}{\lambda_1} \right]^t \frac{1}{\sqrt{2\pi\sigma^2t}} \int_{-\infty}^{\infty} \liminf_{\varepsilon \rightarrow 0} e^{-\frac{(x_0-y)^2}{2\sigma^2t}} e^{-\frac{(c(\varepsilon)-\mu)(x_0-y)}{\sigma^2}} \mathbf{z}_0(y) dy \quad (104)$$

$$= \left[\frac{\mathbf{B}_0}{\lambda_1} \right]^t \frac{1}{\sqrt{2\pi\sigma^2t}} \int_{-\infty}^{\infty} e^{-\frac{(x_0-y)^2}{2\sigma^2t}} e^{-\frac{(c-\mu)(x_0-y)}{\sigma^2}} \mathbf{z}_0(y) dy. \quad (105)$$

From Assumption A5'', $\mathbf{z}_0(y) = (\mathbf{p}_0 \circ \mathbf{r}) e^{-\frac{(c-\mu)}{\sigma^2}y}$. Thus, by the same calculations used in (86)–(87) for the super-solution

$$\mathbf{z}_t(x_0 + ct) \geq \left[\frac{\mathbf{B}_0}{\lambda_1} \right]^t (\mathbf{p}_0 \circ \mathbf{r}) e^{-\frac{(c-\mu)}{\sigma^2}x_0}. \quad (106)$$

From Lemma B.2, see Appendix B for details, we see that

$$\lim_{t \rightarrow \infty} \left[\frac{\mathbf{B}_0}{\lambda_1} \right]^t = \mathbf{r}\ell, \quad (107)$$

where \mathbf{r} and ℓ are the right and left eigenvectors corresponding to λ_1 respectively where the ℓ is normalized by $\langle \ell^T, \mathbf{r} \rangle$. Thus,

$$\lim_{t \rightarrow \infty} \mathbf{z}_t(x_0 + ct) \geq \lim_{t \rightarrow \infty} \left[\frac{\mathbf{B}_0}{\lambda_1} \right]^t (\mathbf{p}_0 \circ \mathbf{r}) e^{-\frac{(c-\mu)}{\sigma^2}x_0} \quad (108)$$

$$= \mathbf{r} \ell (\mathbf{p}_0 \circ \mathbf{r}) e^{-\frac{(c-\mu)}{\sigma^2} x_0} \tag{109}$$

$$= e^{-\frac{(c-\mu)}{\sigma^2} x_0} \mathbf{r} p. \tag{110}$$

Asymptotically, our sub-solution is bounded below by a proportion of the traveling wave for the linear equation where $p = \ell (\mathbf{p}_0 \circ \mathbf{r})$. Since our super-solution satisfies

$$\lim_{t \rightarrow \infty} \mathbf{w}_t(x_0 + ct) \leq e^{-\frac{(c-\mu)}{\sigma^2} x_0} \mathbf{r} p, \tag{111}$$

and our sub-solution satisfies

$$\lim_{t \rightarrow \infty} \mathbf{z}_t(x_0 + ct) \geq e^{-\frac{(c-\mu)}{\sigma^2} x_0} \mathbf{r} p \tag{112}$$

it follows that

$$\lim_{t \rightarrow \infty} \mathbf{v}_t(x_0 + ct) = e^{-\frac{(c-\mu)}{\sigma^2} x_0} \mathbf{r} p. \tag{113}$$

The proof of Theorem 3.3 is complete. □

4 Numerical simulations

In this section, we illustrate the theory of Sect. 3 with a numerical example. All simulations were done using the fast Fourier transform technique (Cooley and Tukey 1965). This method is better than classical quadrature because it speeds up the numerical process from $O(n^2)$ to $O(n \log(n))$.

We begin with a two-stage population model of juveniles, J , and adults, A . The equations in this model are given below,

$$\begin{aligned} J_{t+1}^i(x) &= \int_{-\infty}^{\infty} k(x-y)\zeta(1-m)J_t^i(y) dy \\ &\quad + \int_{-\infty}^{\infty} k(x-y)f_0 e^{-\sum_{i=1}^n (J_t^i(y)+A_t^i(y))} A_t^i(y) dy, \tag{114} \\ A_{t+1}^i(x) &= \int_{-\infty}^{\infty} k(x-y)\zeta m J_t^i(y) dy + \int_{-\infty}^{\infty} k(x-y)\zeta A_t^i(y) dy, \end{aligned}$$

where

$$k(x-y) = \frac{1}{\sqrt{2\pi\sigma^2}} e^{-\frac{(x-y)^2}{2\sigma^2}}. \tag{115}$$

The demography in (114) follows a classical model for biological invasions (Neubert and Caswell 2000), but we assume Gaussian dispersal to align with the assumptions in our theorems. In (114), ζ is the probability of survival to the next generation, m is

the probability of maturation from a juvenile to an adult, f_0 is the number of juveniles produced by an adult in the absence of density-dependent effects. All individuals are assumed to disperse according to a Gaussian dispersal kernel. The growth function for adults producing juveniles is assumed to be a Ricker type growth function where the nonlinearity depends on the density of both juveniles and adults. In the juvenile equation of (114), juveniles can remain juveniles if they survive and do not mature and adults from location y can produce juveniles that disperse to location x . In the adult equation of (114), juveniles become adults if they survive and mature, and adults remain adults if they survive from the previous year.

Let

$$\mathbf{v}_t^i(x) = \begin{bmatrix} J_t^i(x) \\ A_t^i(x) \end{bmatrix}, \tag{116}$$

$$\mathbf{K}(x - y) = \begin{bmatrix} \frac{1}{\sqrt{2\pi\sigma^2}} e^{-\frac{(x-y)^2}{2\sigma^2}} & \frac{1}{\sqrt{2\pi\sigma^2}} e^{-\frac{(x-y)^2}{2\sigma^2}} \\ \frac{1}{\sqrt{2\pi\sigma^2}} e^{-\frac{(x-y)^2}{2\sigma^2}} & \frac{1}{\sqrt{2\pi\sigma^2}} e^{-\frac{(x-y)^2}{2\sigma^2}} \end{bmatrix}, \text{ and} \tag{117}$$

$$\mathbf{B}(\mathbf{u}_t(y)) = \begin{bmatrix} \zeta(1 - m) & f_0 e^{-\sum_{i=1}^n (J_t^i(y) + A_t^i(y))} \\ \zeta m & \zeta \end{bmatrix}. \tag{118}$$

Then we can write (114) in the matrix and vector notation provided in (4).

First, let us verify that the assumptions of Theorems 3.2 and 3.3 are satisfied. Recall that Assumptions A1–A3 and A4' are the same for these two theorems. For Assumption A1, it is clear that our population projection matrix, $\mathbf{B}(\mathbf{u}_t(y))$, is nonnegative from (118) since $\zeta, m, f_0 > 0$. We can calculate \mathbf{B}_0 to be

$$\mathbf{B}_0 = \begin{bmatrix} \zeta(1 - m) & f_0 \\ \zeta m & \zeta \end{bmatrix}. \tag{119}$$

Thus, \mathbf{B}_0 is primitive. For Assumption A2, the dominant eigenvalue of \mathbf{B}_0 is greater than one if

$$f_0 > \frac{(1 - \zeta)(1 - \zeta(1 - m))}{\zeta m}. \tag{120}$$

For details of this calculation see Proposition 3.1 of Marculis and Lui (2016). Since $e^{-\sum_{i=1}^n (J_t^i(y) + A_t^i(y))} \leq 1$ we have $\mathbf{B}(\mathbf{u}_t(y))\mathbf{v} \leq \mathbf{B}_0\mathbf{v}$ for all $\mathbf{v} \geq 0$ and Assumption A3 is satisfied. Even though our operator is not order preserving because of the over-compensation in the Ricker function, Proposition 3.1 in Li et al. (2009) suggests that the calculation for the spreading speed should still hold true. Assumption A4' is clear from the definition of (117). Finally, if we assume our initial condition to decay faster than $e^{-\frac{c-\mu}{\sigma^2}x}$, then the neutral fractions will satisfy Assumption A5' of Theorem 3.2 and we can see that (114) has a unique positive steady state given by

$$J^* = \frac{1 - \zeta}{\zeta m} A^* \text{ and } A^* = -\ln \left(\frac{(1 - \zeta)(1 - \zeta(1 - m))}{f_0 \zeta m} \right), \tag{121}$$

see again Proposition 3.1 of Marculis and Lui (2016). In our numerical simulations the only neutral fraction that does not decay faster than $e^{-\frac{c-\mu}{\sigma^2}x}$ is the one at the leading edge because it was chosen to have an initial form of the traveling wave solution with $c = c^*$. It should be mentioned here that since we are solving this problem numerically it is solved on a finite domain and this is only an approximation to the solution. Therefore, in the moving half-frame, the only neutral fractions that we see are the ones initially at the leading edge. The neutral fractions at the leading edge do not satisfy the exact Assumption A5'' of Theorem 3.3, but asymptotically they decay like $e^{-\frac{c-\mu}{\sigma^2}x}$. However, the asymptotic proportion calculated from Theorem 3.3 agrees with the numerical simulation suggesting that this result should be able to extend to a wider array of initial conditions.

We provide some numerical simulations to see the neutral genetic patterns produced by (114). We begin by running a simulation where the juvenile and adult populations have the same initial distribution as seen in Fig. 1a. This simulation shows that the spread of both juveniles and adults is dominated by the neutral fraction at the leading edge as seen in Fig. 1b. Switching the ordering of the neutral fractions behind the leading edge does not affect the asymptotic behavior in the moving frame. This observation is consistent with the founder effect. The simulations seen in Fig. 1 agree with the results of Theorems 3.2 and 3.3.

For our next simulation, we consider the case where the distribution of the neutral fractions of juveniles and adults do not appear in the same order. This is seen in Fig. 2a. Here we keep the same initial distribution of juvenile individuals as in Fig. 1a, but the initial distribution of adult neutral fractions is assorted differently. In Fig. 2a we can see that initially the neutral fractions at the leading edge of the juvenile and adult populations are light gray and red respectively. Figure 2b shows the distribution of neutral fractions at $t = 100$. At the leading edge the spread is dominated by the

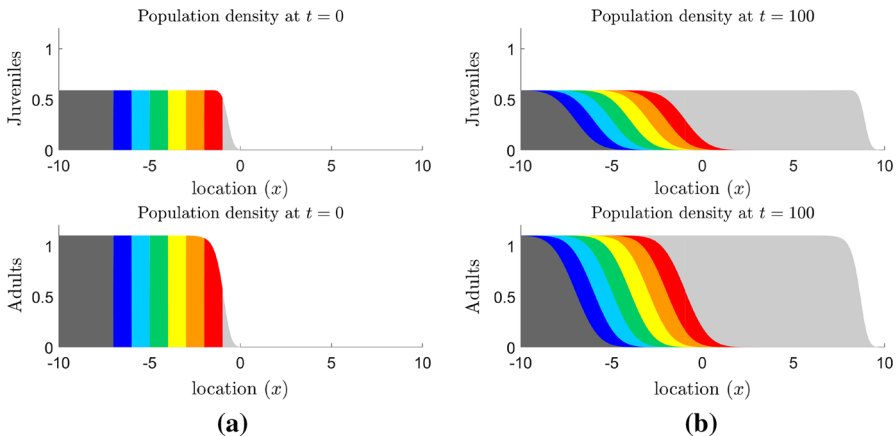


Fig. 1 Numerical realization of (114) for the parameter values $\sigma^2 = 0.01$, $\mu = 0$, $\zeta = 0.7$, $m = 0.8$, and $f_0 = 2.5$ for $n = 8$ neutral fractions. In **a** the plots are the initial conditions for the juvenile and adult populations. Notice that the distribution of neutral fractions for juvenile and adult populations have the same order. In **b** we plot the densities of the juvenile and adult neutral fractions at $t = 100$

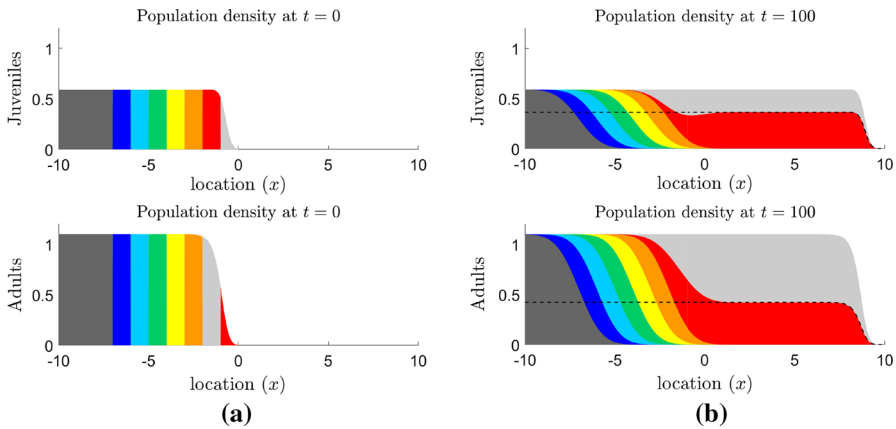


Fig. 2 Numerical realization of (114) for the parameter values $\sigma^2 = 0.01$, $\mu = 0$, $\zeta = 0.7$, $m = 0.8$, and $f_0 = 2.5$ for $n = 8$ neutral fractions. For these parameters $\mathbf{u}^* = (J^*, A^*) = (0.5900, 1.1013)$. In **a** the plots are the initial conditions for the juvenile and adult population. Notice that the distribution of the first two neutral fractions is different for juveniles and adults. The plots in **b** are the densities of the juvenile and adult neutral fractions at $t = 100$. The neutral genetic pattern produced here is due to the difference in the initial distribution of neutral fractions for juveniles and adults. The dashed lines in **b** are calculated from Theorem 3.3, they represent the proportions of red juveniles and adults. Behind the leading edge the proportions are $p^2 J^* = 0.3629$ for juveniles and $p^1 A^* = 0.4238$ for adults

light gray and red neutral fractions. This simulation agrees with our theoretical results because Theorem 3.2 and 3.3 suggest that the spread should be dominated by the neutral fractions that are initially at the leading edge of the population. Again we see that the neutral fractions behind the leading edge do not contribute to the asymptotic spread.

5 Discussion

The main objective of this work is to understand the effect that stage-structure has on the neutral genetic composition of expanding populations as outlined in Sect. 1. We derived the model for the inside dynamics of a stage-structured integrodifference equation in Sect. 2.1. Section 2.2 describes five of our main assumptions related to demography and dispersal. Four of these assumptions are related to the population projection matrix and the fifth is related to the form of the dispersal kernel.

The three main results of the paper are provided in Sect. 3, with their respective proofs in Sect. 3.3. Theorem 3.1 is our first main result, which provides sufficient conditions for a neutral fraction to converge uniformly to zero in the moving half-frame. The five assumptions that must be satisfied are as follows: the population projection matrix must be nonnegative, the population projection matrix evaluated at zero must be primitive and its dominant eigenvalue must be greater than one, the population projection matrix must be maximal at the trivial steady state, all dispersal kernels must be thin-tailed, and the initial condition must satisfy the decay assumption given in Lemma B.1. It should be noted that the Dirac delta function is a thin-tailed disper-

sal kernel and thus we can consider cases where there is no dispersal between some transitions making this theorem very general in terms of the dispersal assumptions.

The second main result is Theorem 3.2. Similar to Theorem 3.1, this theorem also shows conditions under which each neutral fraction converges uniformly to zero in the moving half-frame. The difference with this theorem is that we make a stronger assumption on the dispersal kernels in exchange for a weaker condition on the initial condition. In particular, we assume that all dispersal kernels are Gaussian with identical means and variances. Due to this assumption, we are then able to relax the decay condition on the initial condition of the population to be slightly weaker than is required for Theorem 3.1. The proof for Theorem 3.2 is more elegant than the proof for Theorem 3.1. However, this comes at some cost in the biological realism of the model since it is not common for all stages and transitions to disperse exactly via a Gaussian distribution.

The final result is given in Theorem 3.3. The first four assumptions of this theorem are the same as Theorem 3.2. The fifth assumption assumes that the initial condition decays according to the traveling wave ansatz for the linear equation. Under these assumptions, we are able to asymptotically calculate the proportion that each neutral fraction approaches in the moving frame. This proportion is dependent on the right and left eigenvectors of the population projection matrix evaluated at zero and the initial proportion of each neutral fraction at the leading edge. The proof relies on the construction of super- and sub-solutions to the system. The super-solution, as expected, is chosen to be the linearization of our operator while the sub-solution is defined in a piecewise manner to lie below the nonlinearities. Since all dispersal kernels were assumed to be identical Gaussian distributions, the proportion calculated by Theorem 3.3 does not apply when some stages and transitions do not disperse in the same way.

After completion of the mathematical results, we performed some numerical simulations in Sect. 4 to compare our analytical results to a reasonable biological model. We chose to look at a classical two-stage juvenile adult model where dispersal occurs between all stages and transitions. The first simulation, in Fig. 1, shows that the spread is dominated by the neutral fraction at the leading edge which is an extreme version of the founder effect. However, since we are working with a system of equations, it is possible for the initial distribution of neutral fractions in the juvenile and adult stages to be different. This is seen in Fig. 2a. As predicted from Theorem 3.2, in Fig. 2b, we see that all neutral fractions, except the ones at the leading edge of the juvenile and adult populations, converge uniformly to zero in the moving half-frame. The asymptotic proportions for the two neutral fractions that were initially at the leading edge of the juvenile and adult populations are given by the formula in Theorem 3.3 and plotted as the dashed line in Fig. 2b.

As expected, some of the same results obtained here are similar to those for the scalar population model. That is, Theorems 3.1 and 3.2 are equivalent to their scalar counterparts, Theorem 3 and Theorem 1 respectively, given in Marculis et al. (2017). However, Theorem 3.3 provides a new result for a special case of interacting neutral fractions at the leading edge. This is not possible in the scalar population model. From this theorem, we see the ability for multiple neutral fractions to contribute to the spread of the population. Contributions from multiple neutral fractions to the

population spread are only possible in the scalar model when there is a strong Allee effect (Marculis et al. 2017). Although we would expect similar behavior from our stage-structured model, we are not able to analyze the inside dynamics of a stage-structured model with a strong Allee effect. This is due to the requirement that our results for the strong Allee effect in scalar systems rely on the operator being compact. For a system of equations the necessary theory is more complicated and we were unable to perform this analysis. In the special case where all dispersal kernels are Gaussian with the same mean and variance and all entries of the population projection matrix have the same strong Allee effect type per-capita growth function, then Theorem 2 given in Marculis et al. (2017) can be applied. However, such stringent assumptions would defeat the purpose for considering a stage-structured population model because all stages and transitions would grow and disperse in the same way, essentially reducing the stage-structured model to a scalar equation.

The interesting additional feature that the stage-structured population model offers over scalar models is the ability to have a different initial distribution of neutral fractions for each stage. This difference can lead to multiple neutral fractions driving the spread of the population. Here, we see these dynamics solely for the reason that the initial spatial distribution of neutral fractions is different for each stage.

Several assumptions about the integrodifference dynamics and dispersal kernels limit the applicability of the results in this paper. One limitation to the applicability of our work is seen in Assumption A3. Here we require that our population projection matrix is maximal at zero. This means that we are not considering any kind of demography with Allee effects. In order to prove the asymptotic proportion result seen in Theorem 3.3 we make some restrictive assumptions on the dispersal kernels and initial conditions in the model. Assumption A4' in Theorem 3.3 states that all dispersal kernels are Gaussian with the same mean and variance. This assumption may be unrealistic for many populations because the reason to use a stage-structured population model over a scalar population model is to include differences in demography and dispersal between stages. Assumption A5'' in Theorem 3.3 makes the assumption that the initial conditions are in the form of the traveling wave ansatz for the linear equation. It would be beneficial to generalize Theorem 3.3 for initial conditions that are in the form of the traveling wave solution. The numerical simulations show that we should be able to relax our sixth assumption in our theorems to a more general class of initial conditions. These simulations are not only useful for verifying our mathematical results, but they also provide some insight into opportunities for further mathematical analysis.

Acknowledgements This research was supported by a grant to MAL from the Natural Science and Engineering Research Council of Canada (Grant No. NET GP 434810-12) to the TRIA Network, with contributions from Alberta Agriculture and Forestry, Foothills Research Institute, Manitoba Conservation and Water Stewardship, Natural Resources Canada-Canadian Forest Service, Northwest Territories Environment and Natural Resources, Ontario Ministry of Natural Resources and Forestry, Saskatchewan Ministry of Environment, West Fraser and Weyerhaeuser. MAL is also grateful for support through NSERC and the Canada Research Chair Program. NGM acknowledges support from NSERC TRIA-Net Collaborative Research Grant. JG acknowledges NONLOCAL project (ANR-14-CE25-0013) and the European Research Council (ERC) under the European Unions Horizon 2020 research and innovation programme (Grant agreement No 639638, MesoProbio). The authors also gratefully acknowledge the helpful suggestions from the anonymous reviewers.

A Asymptotic speed of propagation for a system

The following Proposition is taken from Lui (1989a). Let $\beta \in \mathbb{R}^n$ be a positive vector. We define

$$C = \{\mathbf{u} = (u^1, \dots, u^n) \mid \mathbf{0} \leq \mathbf{u}(x) \leq \beta, u^i(x) : \mathbb{R} \rightarrow [0, \beta^i] \text{ is piecewise continuous for } i = 1, \dots, n\}.$$

The operator \mathbf{Q} used in our analytical results is given by

$$\mathbf{Q}[\mathbf{u}] = \int_{-\infty}^{\infty} [\mathbf{K}(x - y) \circ \mathbf{B}(\mathbf{u}(y))] \mathbf{u}(y) dy. \tag{122}$$

Proposition A.1 *Let $\mathbf{Q} = (Q^1, \dots, Q^n) : C \rightarrow C$ satisfy the following conditions:*

- (1) $\mathbf{Q}[\mathbf{0}] = \mathbf{0}$, $\mathbf{Q}[\beta] = \beta$, $\mathbf{0}$ is unstable and β is stable with respect to \mathbf{Q} .
- (2) \mathbf{Q} is translation invariant and has no other fixed-point besides $\mathbf{0}$ and β in C .
- (3) \mathbf{Q} is monotone or order-preserving in C ; that is, if $\mathbf{u} \leq \mathbf{v}$ in C , then $\mathbf{Q}[\mathbf{u}] \leq \mathbf{Q}[\mathbf{v}]$.
- (4) \mathbf{Q} is continuous in the topology of uniform convergence on bounded subsets of \mathbb{R} .
- (5) Let

$$(\mathbf{M}[\mathbf{u}](x))_i = \sum_{j=1}^n \int_{-\infty}^{\infty} \mathbf{u}_j(x - y) m^{ij}(y) dy. \tag{123}$$

be the linearization of \mathbf{Q} at $\mathbf{0}$, where $m^{ij}(y) \geq 0$ is an integrable function. We assume that

$$\mathbf{Q}[\mathbf{u}] \leq \mathbf{M}[\mathbf{u}] \text{ for all } \mathbf{u} \in C. \tag{124}$$

- (6) The matrix $\mathbf{B}(s) = (b^{ij}(s))$, where

$$b^{ij}(s) = \int_{-\infty}^{\infty} e^{sy} m^{ij}(y) dy \tag{125}$$

is irreducible for $0 < s < s^+$.

Let $\rho(s)$ be the dominant eigenvalue of $\mathbf{B}(s)$ and let

$$c^* = \min_{0 < s < s^+} \frac{1}{s} \ln \rho(s). \tag{126}$$

Then c^* is the asymptotic speed of propagation of the operator \mathbf{Q} in the positive direction in the following sense. Let $\mathbf{u}_0 \in C$, \mathbf{u}_0 is non-trivial and vanishes outside of a bounded interval in \mathbb{R} . Let \mathbf{u}_t be defined by $\mathbf{u}_{t+1} = \mathbf{Q}[\mathbf{u}_t]$ for $t = 0, 1, 2, \dots$. Then for any small $\varepsilon > 0$,

$$\lim_{t \rightarrow \infty} \min_{x \leq t(c^* - \varepsilon)} |\mathbf{u}_t(x) - \beta| = 0 \tag{127}$$

$$\text{and } \lim_{t \rightarrow \infty} \max_{x \geq t(c^* + \varepsilon)} |\mathbf{u}_t(x)| = 0. \tag{128}$$

B Mathematical details

The purpose of this section is to provide the mathematical background needed to prove the theorems in Sect. 3. One tool that is used throughout all of our theorems is the reflected Bilateral Laplace transform.

Definition 2 Let $f : \mathbb{R} \rightarrow \mathbb{R}$ where f is piecewise continuous on every finite interval in \mathbb{R} and there exists a $M \in \mathbb{R}^+$ such that $|f(x)| \leq Me^{-sx}$ for all $x \in \mathbb{R}$ and $0 < s < s^+$. Then, the reflected bilateral Laplace transform and its inverse are defined to be

$$F(s) = \mathcal{M}[f(x)] := \int_{-\infty}^{\infty} f(x)e^{sx} dx, \text{ and} \tag{129}$$

$$f(x) = \mathcal{M}^{-1}[F(s)] := \frac{1}{2\pi i} \lim_{R \rightarrow \infty} \int_{\gamma-iR}^{\gamma+iR} F(s)e^{-sx} ds \tag{130}$$

for $0 < s < s^+$, where the integration in Eq. (130) is over the vertical line, $\text{Re}(s) = \gamma$ in the complex plane and γ is greater than the real parts of all singularities of $F(s)$.

By using the convolution theorem, the reflected bilateral Laplace transform can be used to write the solution to our model in terms of the initial condition. This theorem states that the reflected bilateral Laplace transform of a convolution is the product of the reflected bilateral Laplace transforms. That is,

$$\mathcal{M}[f(x) * h(x)](s) = F(s)H(s). \tag{131}$$

Note that the reflected bilateral Laplace transform of a probability density function is also referred to as its moment generating function.

Next, we provide results regarding vector and matrix analysis that are relevant to our subsequent analysis. First, it should be noted that when we write $\mathbf{x} \geq \mathbf{y}$, the inequality is element-wise. That is, $x_i \geq y_i$ for each i . In a similar manner, $\mathbf{x} > \mathbf{y}$ means that $x_i > y_i$ for each i . For the matrix analysis, the following definitions and proposition are needed:

Definition 3 Let $\lambda_1, \dots, \lambda_m$ be the eigenvalues of a matrix \mathbf{A} . Then its spectral radius $\rho(\mathbf{A})$ is defined as:

$$\rho(\mathbf{A}) := \max_{i=1, \dots, m} |\lambda_i|. \tag{132}$$

In other words, the spectral radius of a matrix \mathbf{A} is the modulus of the largest eigenvalue.

Definition 4 A matrix \mathbf{A} is called nonnegative, $\mathbf{A} \geq \mathbf{0}$, if $a_{ij} \geq 0$ for all i, j .

Definition 4 states that a matrix is nonnegative if all elements of the matrix are greater than or equal to zero. Next, we consider primitive matrices.

Definition 5 A nonnegative matrix \mathbf{A} is primitive if there is a positive integer k such that $\mathbf{A}^k > \mathbf{0}$.

Another important concept is that of the dominant eigenvalue of a matrix.

Definition 6 Let $\lambda_1, \dots, \lambda_m$ be the eigenvalues of an $m \times m$ matrix \mathbf{A} . If $|\lambda_1| > |\lambda_j|$ for $j = 2, \dots, m$, then λ_1 is called the dominant eigenvalue of \mathbf{A} .

Next, we discuss the Perron-Frobenius theorem for nonnegative primitive matrices (Bapat and Raghavan 1997).

Proposition B.1 (Perron-Frobenius theorem) *Let $\mathbf{A} \geq \mathbf{0}$ be an $m \times m$ primitive matrix. Then $\mathbf{A}\mathbf{y} = \lambda_1\mathbf{y}$ for some $\lambda_1 > 0$, $\mathbf{y} > \mathbf{0}$ where*

- (i) *The eigenvalue λ_1 is algebraically simple.*
- (ii) *The eigenvalue λ_1 is dominant. That is, for any other eigenvalue μ of \mathbf{A} , $|\mu| < \lambda_1$.*
- (iii) *The only nonnegative eigenvectors of \mathbf{A} are positive scalar multiples of \mathbf{y} .*

By the Perron-Frobenius theorem we know that the spectral radius of a nonnegative primitive matrix is equal to the dominant eigenvalue of that matrix; $\rho(\mathbf{A}) = \lambda_1$. In our analysis we also make use of the Jordan canonical form for square matrices. We use this decomposition because while a nonnegative primitive matrix is not necessarily diagonalizable, every square matrix can none-the-less be written in its Jordan canonical form.

Definition 7 For any square matrix \mathbf{A} , there exists a matrix \mathbf{J} such that

$$\mathbf{A} = \mathbf{P}\mathbf{J}\mathbf{P}^{-1}, \tag{133}$$

where \mathbf{J} is the Jordan canonical form of \mathbf{A} . The Jordan canonical form is a block diagonal matrix

$$\mathbf{J} = \begin{bmatrix} \mathbf{J}_1 & \dots & \mathbf{0} \\ \vdots & \ddots & \vdots \\ \mathbf{0} & \dots & \mathbf{J}_b \end{bmatrix}, \tag{134}$$

where each \mathbf{J}_i is called a Jordan block of \mathbf{A} . For Jordan block i , the diagonal entries are λ_i , the superdiagonal entries are one, and all other entries are zero.

Next, we present two lemmas that were used in the proofs of the main theorems. The first lemma was used in Theorem 3.1 and bounds our initial condition for each neutral fraction i for each stage j , $v_{j,0}^i(x)$, sufficiently to establish the uniform convergence results for the neutral fractions.

Lemma B.1 *Let $x \rightarrow v_{j,0}^i(x)$ satisfy $x^2 v_{j,0}^i(x) e^{sx} \in L^1(\mathbb{R}) \cap L^\infty(\mathbb{R})$, then for each $s > 0$ there exists a positive constant C_j such that*

$$w_{j,0}^i(x) = \frac{C_j e^{-sx}}{1+x^2} \tag{135}$$

bounds $v_{j,0}^i(x)$ for all $x \in \mathbb{R}$. Moreover, the Fourier transform of $w_{j,0}^i(x)e^{sx}$ with respect to x is in $L^1(\mathbb{R})$ and is given by

$$C_j \pi e^{-|\omega|}. \tag{136}$$

For the proof of Lemma B.1, we refer the reader to Lemma 1 by Marculis et al. (2017).

We next provide a lemma that will be used in the proofs of the Theorems 3.2 and 3.3. In particular, we make use of the Jordan canonical form and the Perron-Frobenius theorem outlined above.

Lemma B.2 *Assume that the matrix \mathbf{B}_0 is nonnegative and primitive. Let λ_1 be the dominant eigenvalue of \mathbf{B}_0 , then*

$$\lim_{t \rightarrow \infty} \left[\frac{\mathbf{B}_0}{\lambda_1} \right]^t = \mathbf{r} \boldsymbol{\ell} \tag{137}$$

where \mathbf{r} and $\boldsymbol{\ell}$ are the right and left eigenvectors corresponding to λ_1 respectively with $\boldsymbol{\ell}$ normalized by $\langle \boldsymbol{\ell}^T, \mathbf{r} \rangle$ to account for the scaling in \mathbf{r} .

Proof Writing \mathbf{B}_0 in terms of its Jordan canonical form, we have

$$\lim_{t \rightarrow \infty} \left[\frac{\mathbf{B}_0}{\lambda_1} \right]^t = \lim_{t \rightarrow \infty} \left[\frac{\mathbf{PJP}^{-1}}{\lambda_1} \right]^t \tag{138}$$

$$= \lim_{t \rightarrow \infty} \frac{\mathbf{PJ}^t \mathbf{P}^{-1}}{\lambda_1^t}. \tag{139}$$

Since \mathbf{J} is block diagonal,

$$\mathbf{J}^t = \begin{bmatrix} \mathbf{J}_1^t & \dots & \mathbf{0} \\ \vdots & \ddots & \vdots \\ \mathbf{0} & \dots & \mathbf{J}_b^t \end{bmatrix}. \tag{140}$$

By the Perron-Frobenius theorem there exists a dominant eigenvalue λ_1 of \mathbf{B}_0 because \mathbf{B}_0 is nonnegative and primitive. The first Jordan block is $\mathbf{J}_1 = [\lambda_1]$ and $\mathbf{J}_1^t = [\lambda_1^t]$. For Jordan block j of size $b_j \times b_j$ we have

$$\mathbf{J}_j^t = \begin{bmatrix} \lambda_j^t & \binom{t}{1} \lambda_j^{t-1} & \dots & \binom{t}{b_j-2} \lambda_j^{t-b_j+2} & \binom{t}{b_j-1} \lambda_j^{t-b_j+1} \\ 0 & \lambda_j^t & \dots & \binom{t}{b_j-3} \lambda_j^{t-b_j+3} & \binom{t}{b_j-2} \lambda_j^{t-b_j+2} \\ \vdots & \vdots & \ddots & \vdots & \vdots \\ 0 & 0 & \dots & \lambda_j^t & \binom{t}{1} \lambda_j^{t-1} \\ 0 & 0 & \dots & 0 & \lambda_j^t \end{bmatrix} \tag{141}$$

for $t \geq b_j - 1$. Since $|\lambda_j| < \lambda_1$, using L'Hôpital's rule, we have

$$\lim_{t \rightarrow \infty} \frac{\mathbf{J}_j^t}{\lambda_1^t} = \mathbf{0} \tag{142}$$

for $j = 2, \dots, b$. Returning to the Jordan canonical form,

$$\lim_{t \rightarrow \infty} \frac{\mathbf{J}^t}{\lambda_1^t} = \begin{bmatrix} 1 & \dots & 0 \\ \vdots & \ddots & \vdots \\ 0 & \dots & 0 \end{bmatrix}. \tag{143}$$

Hence from (139),

$$\lim_{t \rightarrow \infty} \frac{\mathbf{P}\mathbf{J}^t\mathbf{P}^{-1}}{\lambda_1^t} = \mathbf{P} \lim_{t \rightarrow \infty} \frac{\mathbf{J}^t}{\lambda_1^t} \mathbf{P}^{-1} \tag{144}$$

$$= \mathbf{P} \begin{bmatrix} 1 & \dots & 0 \\ \vdots & \ddots & \vdots \\ 0 & \dots & 0 \end{bmatrix} \mathbf{P}^{-1} \tag{145}$$

$$= \mathbf{r}\boldsymbol{\ell} \tag{146}$$

because \mathbf{r} is the first column vector of \mathbf{P} and $\boldsymbol{\ell}$ is the first row vector of \mathbf{P}^{-1} . Therefore, from (139) and (146),

$$\lim_{t \rightarrow \infty} \begin{bmatrix} \mathbf{B}_0 \\ \lambda_1 \end{bmatrix}^t = \mathbf{r}\boldsymbol{\ell}. \tag{147}$$

The proof of Lemma B.2 is complete. □

References

Austerlitz F, Garnier-Géré P (2003) Modelling the impact of colonisation on genetic diversity and differentiation of forest trees: interaction of life cycle, pollen flow and seed long-distance dispersal. *Heredity* 90(4):282

Bapat RB, Raghavan TE (1997) Nonnegative matrices and applications, vol 64. Cambridge University Press, Cambridge

Bataillon TM, David JL, Schoen DJ (1996) Neutral genetic markers and conservation genetics: simulated germplasm collections. *Genetics* 144(1):409–417

Bateman AW, Buttenschön A, Erickson KD, Marculis NG (2017) Barnacles versus bullies: modelling biocontrol of the invasive european green crab using a castrating barnacle parasite. *Theor Ecol* 10(3):305–318

Bonnefon O, Garnier J, Hamel F, Roques L (2013) Inside dynamics of delayed travelling waves. *Math Mod Nat Phen* 8:44–61

Bonnefon O, Coville J, Garnier J, Roques L (2014) Inside dynamics of solutions of integro-differential equations. *Discrete Contin Dyn Syst Ser B* 19(10):3057–3085

Cooley JW, Tukey JW (1965) An algorithm for the machine calculation of complex fourier series. *Math Comput* 19(90):297–301

- Cullingham CI, Cooke JE, Dang S, Davis CS, Cooke BJ, Coltman DW (2011) Mountain pine beetle host-range expansion threatens the boreal forest. *Mol Ecol* 20(10):2157–2171
- Davis MB, Shaw RG (2001) Range shifts and adaptive responses to quaternary climate change. *Science* 292(5517):673–679
- Easterling MR, Ellner SP, Dixon PM (2000) Size-specific sensitivity: applying a new structured population model. *Ecology* 81(3):694–708
- Garnier J, Lewis MA (2016) Expansion under climate change: the genetic consequences. *Bull Math Biol* 78(11):2165–2185
- Garnier J, Giletti T, Hamel F, Roques L (2012) Inside dynamics of pulled and pushed fronts. *J Math Pures Appl* 98(4):428–449
- Hallatschek O, Nelson DR (2008) Gene surfing in expanding populations. *Theor Popul Biol* 73(1):158–170
- Hastings A, Cuddington K, Davies KF, Dugaw CJ, Elmendorf S, Freestone A, Harrison S, Holland M, Lambrinos J, Malvadkar U et al (2005) The spatial spread of invasions: new developments in theory and evidence. *Ecol Lett* 8(1):91–101
- Hewitt G (2000) The genetic legacy of the quaternary ice ages. *Nature* 405(6789):907
- Holderegger R, Kamm U, Gugerli F (2006) Adaptive versus neutral genetic diversity: implications for landscape genetics. *Landscape Ecol* 21(6):797–807
- Howe HF, Smallwood J (1982) Ecology of seed dispersal. *Annu Rev Ecol Syst* 13(1):201–228
- Ibrahim KM, Nichols RA, Hewitt GM (1996) Spatial patterns of genetic variation generated by different forms of dispersal during range expansion. *Heredity* 77(3):282
- Kot M, Lewis MA, van den Driessche P (1996) Dispersal data and the spread of invading organisms. *Ecology* 77(7):2027–2042
- Lefkovich L (1965) The study of population growth in organisms grouped by stages. *Biometrics* 21:1–18
- Leslie PH (1945) On the use of matrices in certain population mathematics. *Biometrika* 33(3):183–212
- Levin LA (2006) Recent progress in understanding larval dispersal: new directions and digressions. *Integr Comp Biol* 46(3):282–297
- Lewis MA, Marculis NG, Shen Z (2018) Integrodifference equations in the presence of climate change: persistence criterion, travelling waves and inside dynamics. *J Math Biol* 77(6–7):1649–1687
- Li B, Lewis MA, Weinberger HF (2009) Existence of traveling waves for integral recursions with non-monotone growth functions. *J Math Biol* 58(3):323–338
- Liebold AM, Halverson JA, Elmes GA (1992) Gypsy moth invasion in north america: a quantitative analysis. *J Biogeogr* 19:513–520
- Lubina JA, Levin SA (1988) The spread of a reinvading species: range expansion in the california sea otter. *Am Nat* 131(4):526–543
- Lui R (1982a) A nonlinear integral operator arising from a model in population genetics I monotone initial data. *SIAM J Math Anal* 13(6):913–937
- Lui R (1982b) A nonlinear integral operator arising from a model in population genetics II initial data with compact support. *SIAM J Math Anal* 13(6):938–953
- Lui R (1983) Existence and stability of travelling wave solutions of a nonlinear integral operator. *J Math Biol* 16(3):199–220
- Lui R (1989a) Biological growth and spread modeled by systems of recursions I mathematical theory. *Math Biosci* 93(2):269–295
- Lui R (1989b) Biological growth and spread modeled by systems of recursions II biological theory. *Math Biosci* 93(2):297–311
- Lutscher F, Lewis MA (2004) Spatially-explicit matrix models. *J Math Biol* 48(3):293–324
- Marculis NG, Lui R (2016) Modelling the biological invasion of *carcinus maenas* (the European green crab). *J Biol Dyn* 10(1):140–163
- Marculis NG, Lui R, Lewis MA (2017) Neutral genetic patterns for expanding populations with nonoverlapping generations. *Bull Math Biol* 79(4):828–852
- Moloney KA (1986) A generalized algorithm for determining category size. *Oecologia* 69(2):176–180
- Neubert MG, Caswell H (2000) Demography and dispersal: calculation and sensitivity analysis of invasion speed for structured populations. *Ecology* 81(6):1613–1628
- Pluess AR (2011) Pursuing glacier retreat: genetic structure of a rapidly expanding *larix decidua* population. *Mol Ecol* 20(3):473–485
- Roques L, Hosono Y, Bonnefon O, Boivin T (2015) The effect of competition on the neutral intraspecific diversity of invasive species. *J Math Biol* 71(2):465–489

- Roques L, Garnier J, Hamel F, Klein EK (2012) Allee effect promotes diversity in traveling waves of colonization. *Proc Natl Acad Sci* 109(23):8828–8833
- Vandermeer J (1978) Choosing category size in a stage projection matrix. *Oecologia* 32(1):79–84
- Veit RR, Lewis MA (1996) Dispersal, population growth, and the allee effect: dynamics of the house finch invasion of eastern North America. *Am Nat* 148(2):255–274
- Weinberger HF (1978) Asymptotic behavior of a model in population genetics. In: *Nonlinear Partial Differential Equations and Applications*, Springer, pp 47–96
- Weinberger HF (1982) Long-time behavior of a class of biological models. *SIAM J Math Anal* 13(3):353–396

Publisher's Note Springer Nature remains neutral with regard to jurisdictional claims in published maps and institutional affiliations.